Bound-Electron–Lattice Coupling and Vibronic Spectra

W. E. BRON
IBM Watson Research Center, Yorktown Heights, New York
(Received 21 July 1965)

The radial extent of the coupling between the bound electronic states of a defect ion in a crystal and the vibrations of the lattice ions is investigated. An electrostatic-coupling model is used to evaluate the electron-lattice interaction. It is found that those electronic transitions which involve a change in configuration are coupled primarily to the vibrations of ions in the immediate vicinity of the defect. Consequently, if there exist local or pseudolocalized vibrations, the resultant vibronic spectra are dominated by transitions to vibrational modes which have high local amplitude. In contrast, it is found that in general, electronic transitions within a configuration are coupled to nonlocalized vibrations as well as to the localized vibrations. In the special case of the transition $^5D_0 \rightarrow {}^7F_0$ of Sm^{2+}, the coupling is primarily to nonlocalized vibrations, so that the vibrations resemble those of ions of the undisturbed lattice. The observed vibronic structure accompanying this transition of Sm^{2+} in the alkali halides is presented. A comparison is made for Sm^{2+}:KBr between the singularities in the phonon density of states as observed in the vibronic structure, and those predicted from the published dispersion curves of KBr obtained from neutron-scattering data. The agreement is found to be very good. The vibronic structure accompanying the same transition of Sm^{2+} in the alkaline-earth halides is also discussed.

I. INTRODUCTION

THIS paper is concerned with an investigation of the radial extent of the coupling between bound electronic states of a defect ion in a crystal and the vibrations of ions in the host lattice. The interaction will be discussed in terms of the electrostatic-coupling model introduced previously.[1] We make use of this model to explain the origin of the fact that two types of vibronic spectra accompany transitions between pure electronic states of transition-metal ions and rare-earth metal ions dissolved in ionic host lattices. The first type consists of long series of sharp, essentially evenly spaced lines which are observed together with electronic transitions involving a change in configuration (interconfiguration), as e.g., the transitions $4f^n \rightleftarrows 4f^{n-1}5d$ in rare-earth ions.[2–5] In contrast, the vibronic structure accompanying transitions of the type $4f^n \rightleftarrows 4f^n$ or $3d^n \rightleftarrows 3d^n$ (intraconfiguration) consists of a limited set of comparatively broad bands without a constant frequency interval.[3–6]

In two recent papers[1,2] we have analyzed in detail the vibronic structure observed with interconfiguration transitions of the type $4f^n \rightleftarrows 4f^{n-1}5d$ of Sm^{2+}, Eu^{2+}, and Yb^{2+} in the alkali halides. We have shown that the sharp-line vibronic structure arises from a coupling to pseudolocalized vibrations which arise in the vicinity of the rare-earth ion.

The vibronic structure accompanying intraconfiguration transitions has normally been assigned to coupling to nonlocalized vibrational modes, i.e., modes which approximate the motion of the undisturbed lattice. In fact, it has become fashionable to assign peaks in this structure to peaks in the density of lattice vibrational states. This has been done, even though the mass and electronic structure of the optically active ion are often considerably different from those of the host lattice, as e.g., transition-metal ions in MgO. Thus one suspects that localized, or at least pseudolocalized, vibrational modes exist in the vicinity of the optically active ion.

The intraconfiguration transitions of Sm^{2+} can be observed optically in a different region of the spectrum from the interconfiguration transitions. The vibronic structure on the $4f^6 \rightarrow 4f^6$ transitions have the broad-line structure described above, even though the interconfiguration transitions have vibronic structure clearly due to pseudolocalized vibrations. This implies that two different types of coupling can exist simultaneously. That is, for interconfiguration transitions the coupling is predominantly localized, whereas for intraconfiguration transitions there is an extended coupling predominantly to the vibrations of lattice ions sufficiently removed from the defect. The vibronic structure accompanying intraconfiguration transitions would, therefore, provide a relatively simple means of studying the density of states of phonons, if this assignment of the origin of the vibronic spectrum is correct.

In Ref. 1 we have introduced the electrostatic-coupling model. Here we investigate the radial extent of this coupling, in order to clarify the origin of the two types of vibronic spectra described above. Although it will become necessary in the present paper to discuss the range of the coupling in terms of simplified defects and lattices, the ultimate aim is to apply the results to

[1] W. E. Bron and M. Wagner, Phys. Rev. **139**, A233 (1965).
[2] M. Wagner and W. E. Bron, Phys. Rev. **139**, A223 (1965).
[3] J. D. Axe and P. P. Sorokin, Phys. Rev. **130**, 945 (1963).
[4] D. L. Wood and W. Kaiser, Phys. Rev. **126**, 2079 (1962).
[5] See also, e.g., P. P. Sorokin, M. J. Stevenson, J. R. Lankard, and G. D. Pettit, Phys. Rev. **127**, 503 (1962); A. A. Kaplyanskii and P. P. Feofilov, Opt. i Spektroskopia **13**, 235 (1962) [English transl.: Opt. Spectry (USSR) **13**, 129 (1962)]; M. D. Sturge, Phys. Rev. **130**, 639 (1963); A. A. Kaplyanskii and P. P. Feofilov, Opt. i Spektroskopia **16**, 264 (1964) [English transl.: Opt. Spectry. (USSR) **16**, 144 (1964)]; A. I. Ryskin, G. I. Khilko, B. I. Maksakov, and K. K. Dubenskii, *ibid.* p. 274.
[6] See also, e.g., I. Richman, R. A. Satten, and E. Y. Wong, J. Chem. Phys. **39**, 1833 (1963); G. F. Imbush, W. M. Yen, A. L. Schawlow, D. E. McCumber, and M. D. Sturge, Phys. Rev. **133**, A1029 (1964); W. M. Yen, W. C. Scott, and A. L. Schawlow, *ibid.* **136**, A271 (1964); M. V. Hobden, Phys. Letters **15**, 10 (1965).

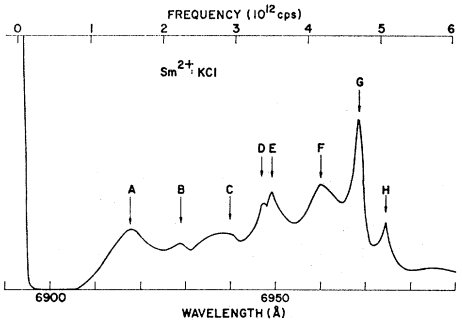

FIG. 1. Vibronic structure and the pure electronic transition $^5D_0 \rightarrow {}^7F_0$ (at 6892.8 Å) of Sm^{2+}:KCl at 10°K.

the real cases of Sm^{2+} in the alkaline-earth halides and in the alkali halides, particularly Sm^{2+}:KBr. The latter is important because it is possible to compare the vibronic structure with the phonon dispersion curves of the KBr lattice obtained by Woods *et al.*[7] from neutron-scattering data. We include, therefore, the experimental results on the vibronic structure accompanying the $4f^6 \rightarrow 4f^6$ transitions of Sm^{2+} in the alkali halides, which have not been previously reported.

II. EXPERIMENTAL METHODS AND RESULTS

The general experimental techniques have been given elsewhere.[2,8] Emission spectra due to transitions between pure electronic states of the $4f^6$ configuration of Sm^{2+} in KCl, RbCl, and KBr at 10°K have been given in Ref. 8 together with a detailed analysis of the pertinent states. Very weak vibronic structure can be observed with most of the pure electronic transitions. However, only with the transition $^5D_0(A_1) \rightarrow {}^7F_0(A_1)$ is the vibronic structure sufficiently intense to make reasonable resolution of its structure possible. In general, the peak intensity of the vibronic structure is roughly two orders of magnitude lower than those of the pure electronic transitions.

Figures 1–3 show the vibronic structure accompanying the transition $^5D_0(A_1) \rightarrow {}^7F_0(A_1)$ which appears near 6890 Å. Table I lists the frequency differences between the various vibronic peaks and the position of the pure electronic line. As pointed out earlier, this vibronic structure consists of relatively broad lines without a constant frequency interval. The half-width of these lines is about 5 Å or larger. In contrast, we show in Fig. 4 the vibronic structure which appears on the lowest energy absorption band of Sm^{2+} in KBr, which is due to transitions of the type $4f^6 \rightarrow 4f^5 5d$. The vibronic structure for these transitions clearly involves a number of series of narrow lines (half-widths are typically less than 5 Å) with essentially constant frequency interval. The reader is referred to Ref. 2 for more details on this type of structure.

TABLE I. Peak positions of vibronic bands (in units of 10^{12} sec^{-1}).

KCl Peak designation	ν	RbCl Peak designation	ν	KBr Peak designation	ν
A	1.58	*A*	1.36	*A*	1.26
B	2.27	*B*	2.00	*B*	2.21
C	2.94	*C*	2.61	*C*	2.57
D	3.42	*D*	3.60	*D*	3.18
E	3.54	*E*	4.08	*E*	3.57
F	4.22	*F*	4.21	*F*	4.38
G	4.72				
H	5.08				

III. DISCUSSION

In Sec. IIIA of this discussion, we formulate the electron-lattice coupling parameters and show how these may be evaluated in terms of the electrostatic-coupling model. In terms of this model the coupling has been shown[1] to be proportional to the projection of the field of the charge distribution of the electrons of the defect ion onto the vibrational eigenvectors of the lattice ions. We further show that, in general, the coupling involves both the even- and odd-parity components of the electron-lattice interaction potential. In Sec. IIIB, we evaluate these even- and odd-parity components and show that the even part involves a coupling primarily to pseudolocalized vibrations, while the odd part involves a coupling dominated by nonlocalized vibration. We further show that, in general, interconfiguration transitions are coupled predominantly to the even part of the potential, i.e., to localized vibrations. Whereas, in general, both types of coupling must be considered in intraconfiguration transitions. In Sec. IIIC we analyze the special case of the intraconfiguration transition $^5D_0 \rightarrow {}^7F_0$ of Sm^{2+} for which the even coupling vanishes, and show that for it the vibronic structure approximates a part of the density of states of the vibrations of the undisturbed lattice.

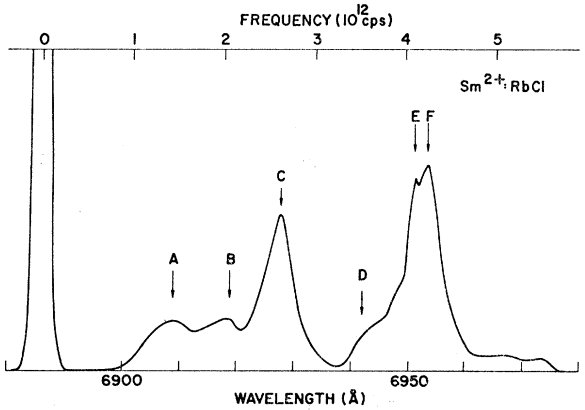

FIG. 2. Vibronic structure and the pure electronic transition $^5D_0 \rightarrow {}^7F_0$ (at 6886.4 Å) of Sm^{2+}:RbCl at 10°K.

[7] A. D. B. Woods, B. N. Brockhouse, R. A. Cowley, and W. Cochran, Phys. Rev. **131**, 1025 (1963).
[8] W. E. Bron and W. R. Heller, Phys. Rev. **136**, A1433 (1964).

A. Electron-Lattice Coupling Parameters

Within the Born-Oppenheimer approximation,[9] we write the total wave function for the coupled electron-lattice system as

$$\Psi(r,Q)=\psi(r,Q)\phi(Q), \tag{1a}$$

where ψ, the electronic wave function, is a function of the electron coordinates (r) and nuclear normal mode (Q) coordinates, and ϕ is the nuclear wave function. Further, under the Franck-Condon principle, that the positions of the nucleii remain fixed during an electronic transition, we may write the probability of a dipole transition between electron-lattice states as[1]

$$\langle\Psi_{j'n'}|P_\epsilon|\Psi_{jn}\rangle=\langle\psi_j|P_\epsilon|\psi_j\rangle \times\langle\phi_{j'n'}(Q_\kappa{}^j-\alpha_\kappa{}^{j'j})|\phi_{jn}(Q_\kappa{}^j)\rangle, \tag{1b}$$

where P_ϵ is the electric-dipole operator, ψ_j the electronic eigenfunction for the state j, ϕ_{jn} the nuclear eigenfunction when the system is in the jth electronic state and the nth nuclear vibrational state, and $\alpha_\kappa{}^{j'j}$ is the change in the equilibrium position of the κth normal coordinate between the jth and j'th electronic state.

The displacement parameter α_κ, between the electronic state j' and j, can be shown to be[1]

$$\alpha_\kappa{}^{j'j}=(1/\omega_\kappa{}^2)[\langle\psi_{j'}|U_\kappa|\psi_{j'}\rangle-\langle\psi_j|U_\kappa|\psi_j\rangle], \tag{2}$$

where ω_κ is the vibrational frequency of the κth normal mode, and U_κ is the coefficient of Q_κ in the expansion of the interaction potential $U(r,Q)$, between the defection electrons and all the lattice ions. The quadratic term in this expansion leads to a change in the vibrational frequency in the two electronic states and to a mixing of modes. However, in accordance with the experimental observation that such changes are very small,[2] we shall consider only the effect of the linear term. It is important to note that we have adopted here, for the sake of simplicity, what amounts to the "zero-order" Born-Oppenheimer approximation.[1] Also, to avoid the complication of the Jahn-Teller effect we will assume, for the time being, that the electronic states are nondegenerate. For a clear discussion of these complications we refer the reader to a paper of Longuet-Higgins.[10]

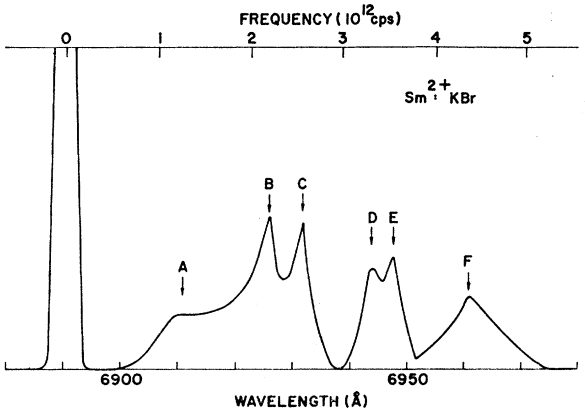

FIG. 3. Vibronic structure and the pure electronic transition ${}^5D_0\rightarrow{}^7F_0$ at (6891.0 Å) of Sm^{2+}:KBr at 10°K.

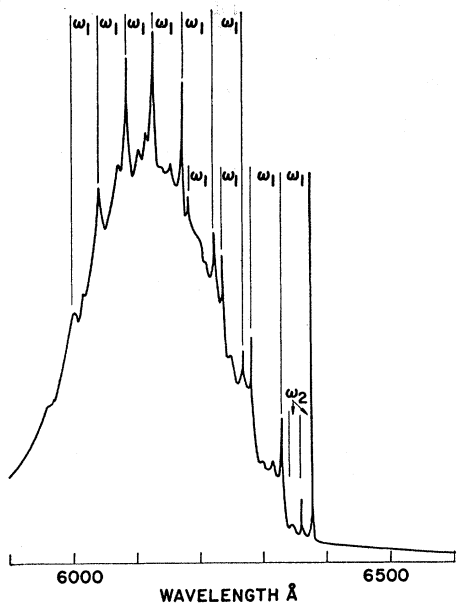

FIG. 4. Vibronic structure on the lowest energy absorption band due to $4f^6\rightarrow4f^55d$ transitions in Sm^{2+}:KBr at 10°K. The intervals between the sharp vibronic lines are indicated by ω_1 and ω_2. These two vibrational frequencies are discussed in detail in Refs. 1 and 2.

From Eq. (1) it is clear that, for finite transition probabilities, $\psi_j{}^*\psi_j$ must have odd-parity components, since P_ϵ is odd. If in addition α_κ is finite, then one or more quanta of vibrational energy can be emitted or absorbed together with the pure electronic transition. The transition probability $|\langle\phi_m(Q_\kappa{}^j-\alpha_\kappa{}^{j'j})|\phi_0(Q_\kappa{}^j)\rangle|^2$ from a state with zero vibrational quanta in the κth mode to one with m vibrational quanta has been shown to be,[1,11]

$$P_\kappa{}^m=(1/m!)[\omega_\kappa\alpha_\kappa{}^2/2h]^m. \tag{3}$$

From the above, we note that the electron-lattice interaction is characterized by the "linear" coupling term $\langle\psi_j|U_\kappa|\psi_j\rangle Q_\kappa$ and by the displacement parameter α_κ; the former, as we shall see, describes the strength and radial extent of the electron-lattice coupling, and the latter [through Eq. (3)] characterizes the structural form of the experimentally observable vibronic structure.

In Ref. 1 we have defined a point-ion, electrostatic-coupling model. Here we apply this model to evaluate the linear coupling, which for the jth electronic state can be written as

$$\sum_l \rho eZ_l[\mathbf{F}_j(\mathbf{R}_l)\cdot\mathbf{u}_l], \tag{4}$$

[9] M. Born and J. R. Oppenheimer, Ann. Physik 84, 457 (1927).

[10] H. C. Longuet-Higgins, Advan. Spectry. 2, 429 (1961).

[11] M. Wagner, J. Chem. Phys. 41, 3939 (1964).

TABLE II. Axial components of dipole moment and quadrupole tensor for the first three states of Ce^{3+}.

State	P_z	Q_{zz}
$\|4f,2,F,\frac{5}{2},\frac{1}{2}\rangle$, A		$0.12\langle 4f\|r^2\|4f\rangle$
$\|4f,2,F,\frac{7}{2},\frac{1}{2}\rangle$, B	$-0.20\langle 4f\|r\|5d\rangle$	$-0.18\langle 4f\|r^2\|4f\rangle$
$\|5d,2,D,\frac{5}{2},\frac{1}{2}\rangle$, C	$-0.20\langle 4f\|r\|5d\rangle$	$0.80\langle 5d\|r^2\|5d\rangle$

where ρ is an effective dielectric constant for the lattice ions, here assumed to be point charges of strength Z_l whose position in the lattice is given by the sum of the vector $\mathbf{R}_l$ defining their equilibrium position and $\mathbf{u}_l$ which gives the displacement from that position. $\mathbf{F}_j(\mathbf{R}_l)$ is the electric field, due to the charge distribution $|\psi_j^*\psi_j|$, evaluated at the nuclear equilibrium positions, and e the electronic charge. Specifically, the field is given by

$$\mathbf{F}_j(\mathbf{R}_l)=e\int\psi_j^*\sum_s\frac{r_s-R_l}{|\mathbf{r}_s-\mathbf{R}_l|^3}\psi_j\prod_s d^3r_s, \tag{5}$$

where the sum extends over all s electrons not in closed shells of the defect ion. The electrostatic field $\mathbf{F}_j$ can be expanded into multipole components, i.e., into monopole, dipole, quadrupole, etc. terms.

Substituting (4) into (2) we obtain for the κth mode

$$\alpha_\kappa=\frac{\rho e}{\omega_\kappa^2}\sum_l Z_l[\mathbf{F}_{j'}(\mathbf{R}_l)-\mathbf{F}_j(\mathbf{R}_l)]\cdot\zeta_\kappa, \tag{6}$$

where ζ_κ are vibrational normal modes. Since the monopole terms of $\mathbf{F}_j$ are not functions of the electronic state, they cancel in (6) for distances outside of the electronic charge distribution. The reader is referred to Ref. 1 for a more detailed discussion of the coupling parameters and of the electrostatic-coupling model.

An evaluation of the electron-lattice coupling is accordingly reduced to the determination of the fields $\mathbf{F}_j(\mathbf{R}_l)$ and the vibrational eigenvectors. For the fields we require the electronic wave functions ψ_j which we shall discuss, for the sake of clarity, in terms of a hypothetical free ion which has, among other states, the following three electronic states:

State A: the ground state, which belongs to a configuration which has a parity α.

State B: an excited state, but still of the ground configuration, i.e., of parity α.

State C: an excited state which is a part of the first excited configuration which has a parity α' opposite to that of α.

The above electronic states are perturbed when this ion is placed in a crystal. When the defect site lacks inversion symmetry, the states are mixed by the odd-parity elements of the crystal field V_c. This case, which corresponds, e.g., to Sm^{2+} in the alkali halides,[8] will hereafter also be referred to as case I. The electronic wave function for the state B can be written as

$$\psi_B=a_B\psi_B(\alpha)-\sum_j\frac{\langle\psi_j(\alpha')\,|\,V_c\,|\psi_B(\alpha)\rangle}{E_j-E_B}\psi_j(\alpha') \tag{7a}$$

and similarly for the states A and C.

The second case (case II) corresponds, e.g., to Sm^{2+} in the alkaline-earth halides for which the defect site has inversion symmetry. For this case opposite-parity states may still be admixed through the odd components of the linear interaction potential $U_\kappa Q_\kappa$. For example, the electronic wave function for the state B in the first-order Born-Oppenheimer approximation is

$$\psi_B(r,Q)=a_B'\psi_B^0(\alpha)-\sum_{\kappa,j}\frac{\langle\psi_j^0(\alpha')\,|\,U_\kappa Q_\kappa\,|\psi_B^0(\alpha)\rangle}{E_j^0-E_B^0}\psi_j^0(\alpha') \tag{7b}$$

and similarly for the states A and C. Here ψ_j^0 are zero-order Born-Oppenheimer wave functions. The vibrational admixture of opposite-parity states can also occur for case I. However, from the observed strength of certain otherwise forbidden electric-dipole transitions of Sm^{2+} in the alkali halides we deduce that the pertinent odd-parity elements of the crystal field are large. Accordingly, we shall assume that, for case I, the admixture via the static crystal fields exceeds that due to the linear interaction potential.

For the case without inversion symmetry (case I) the electric-dipole transition probability for intra- or interconfiguration transition follows directly from Eq. (1), and the displacement α_κ from Eq. (2) which, to terms of first order in V_c becomes

$$\omega_\kappa^2\alpha_\kappa=a_{j'}{}^2\langle\psi_{j'}(\alpha)\,|\,U_\kappa\,|\psi_{j'}(\alpha)\rangle-a_j{}^2\langle\psi_j(\alpha)\,|\,U_\kappa\,|\psi_j(\alpha)\rangle-a_{j'}\sum_i\frac{\langle\psi_i(\alpha')\,|\,V_c\,|\psi_{j'}(\alpha)\rangle}{E_i-E_{j'}}\langle\psi_{j'}(\alpha)\,|\,U_\kappa\,|\psi_i(\alpha')\rangle, \tag{8}$$

where the κth mode can be considered as a sum of even- and odd-parity modes. The first two terms of (8) involve only the even-parity parts of U_κ, i.e., the quadrupole and higher even terms of $\mathbf{F}_j$, whereas the third term of (8) involves only the odd-parity parts of U_κ, i.e., the dipole and higher odd terms of $\mathbf{F}_j$. The monopole parts of $\mathbf{F}_j$, as noted above, do not enter into (8) because the charge distribution $\psi_j^*\psi_j$ for the $4f$ and $5d$ shells of rare-earth ions is strongly localized.

TABLE III. Values of radial integrals for Ce^{3+} and Sm^{2+} (in atomic units).

Radial integral	Ce^{3+}	Sm^{2+}
$\langle 4f\|r^2\|4f\rangle$	1.5	1.5
$\langle 4f\|r\|5d\rangle$	0.9	1.0
$\langle 5d\|r^2\|5d\rangle$	7.0	7.6

TABLE IV. Estimate of axial component of coupling fields of Sm^{2+} (in statvolts/cm).

Electronic state	Dipole field	Dipole field (at $r=1$ Å)	Quadrupole field	Quadrupole field (at $r=1$ Å)
A			$0.06\times10^{-27}r^{-4}$	0.06×10^{5}
B	$-1.9\times10^{-21}r^{-3}$	-1.9×10^{3}	$-0.11\times10^{-27}r^{-4}$	-0.11×10^{5}
C	$-1.9\times10^{-21}r^{-3}$	-1.9×10^{3}	$2.3\times10^{-27}r^{-4}$	2.3×10^{5}

For the case of inversion symmetry (case II), the electric-dipole transition probability becomes, to terms of first order in $U_\kappa Q_\kappa$,

$$\langle\Psi_{j'n'}|P_\epsilon|\Psi_{jn}\rangle=\prod_{\kappa g}\langle\phi_{j'n'}(Q_{\kappa g}{}^{i}-\alpha_\kappa{}^{i'i})|\phi_{jn}(Q_{\kappa g}{}^{i})\rangle$$
$$\times\Bigg\{\langle\psi_{j'}{}^{0}(\alpha)|P_\epsilon|\psi_j{}^{0}(\alpha)\rangle$$
$$-\sum_{\kappa u,i}\langle\phi_{j',n-1}(Q_{\kappa u})|Q_{\kappa u}|\phi_{j,n}(Q_{\kappa u})\rangle$$
$$\times\Bigg[\frac{\langle\psi_{j'}{}^{0}(\alpha)|P_\epsilon|\psi_i{}^{0}(\alpha')\rangle\langle\psi_i{}^{0}(\alpha')|U_{\kappa u}|\psi_j{}^{0}(\alpha)\rangle}{E_i{}^{0}-E_j{}^{0}}$$
$$+\frac{\langle\psi_{j'}{}^{0}(\alpha)|U_{\kappa u}|\psi_i{}^{0}(\alpha')\rangle\langle\psi_i{}^{0}(\alpha')|P_\epsilon|\psi_j{}^{0}(\alpha)\rangle}{E_i{}^{0}-E_{j'}{}^{0}}\Bigg]\Bigg\}, \quad (9)$$

where the subscripts u and g refer to odd and even vibrational modes. The displacement α_κ in (9) is finite only for the even modes, since for case II the charge distribution $|\psi_j{}^*\psi_j|$ is on a time average still even, and can interact only with the even vibrations to give a displacement of the even normal coordinates, $Q_{\kappa g}$. This term, therefore, involves the even parts of F_j. The second term of (9) also involves the even modes, as well as the odd-parity parts of U_κ, i.e., the odd modes.

From Eqs. (7) through (9) we conclude that, in general, intra- and interconfigurational electronic transitions are coupled to both the even- and odd-parity parts of U_κ. In the next section we evaluate the coupling for a sample case, and show that the relative strength of the coupling to the even parts as compared to the odd parts depends on the electronic state, and further that the radial extent of the coupling also differs for the even and odd components of U_κ.

B. Magnitude and Radial Extent of the Coupling

The actual magnitudes of the coupling fields depend on the particular electronic states as shown in Eq. (5). Since our aim is to analyze the electron-lattice coupling for the Sm^{2+} ion, we would need to evaluate Eq. (5) for all the electrons of that ion. This calculation is extremely tedious, and to carry it through would require assumptions as to the states of the $4f^5 5d$ configuration. In order to obtain an order of magnitude estimate of the fields, we determine instead the coupling field for the Ce^{3+} ion which has only one $4f$-shell electron, and for which the states of the $5d$ configuration are known.[12] The calculation is further simplified by assuming a $C_{\infty v}$ site symmetry. Accordingly, the dipole and quadrupole moments of the electronic charge distribution have been evaluated for the states $|4f,2,F,\frac{7}{2},\frac{1}{2}\rangle$ and $|4f,2,F,\frac{5}{2},\frac{1}{2}\rangle$ of Ce^{3+} (here given in the $|4f,S,L,J,J_z\rangle$ notation and which correspond to the states A and B) and for the $|5d,2,D,\frac{5}{2},\frac{1}{2}\rangle$ state (which corresponds to state C). The integration over the angular parts of the wave function is done first. Table II lists the z components of the dipole moment and the zz element of the quadrupole tensor in terms of the radial integrals. Here it is assumed that the ground state is purely of the $4f$ configuration. Values for $\langle 4f|r^2|4f\rangle$ and $\langle 4f|r|5d\rangle$ for Ce^{3+} and Sm^{3+} were obtained by extrapolation and interpolation of the values given in the paper by Judd[13] for Pr^{3+}, Nd^{3+}, Eu^{3+}, and Tm^{3+}. Similarly, values for $\langle 5d|r^2|5d\rangle$ were obtained from the calculations of Rajnak[14] for Pr^{3+} and Tm^{3+}. Estimates of the radial integrals for Sm^{2+} were then obtained by scaling up the values for Sm^{3+} by 20%.[15] Values so obtained are listed in Table III. If one makes the rough approximation that the integration over the angular parts of the wave function, as given in Table II for Ce^{3+}, applies to Sm^{3+}, and uses the values of Table III for the radial integral for Sm^{2+}, one can evaluate the dipole part and the quadrupole part of the coupling field. The component of these fields in the axial direction and their value at $r=1$ Å are given in Table IV for the three electronic states.

An important feature of these results is that the quadrupole field for the state C far exceeds in magnitude all the other fields. This comes about primarily through the increase in the radial integral in going from the ground configuration to an excited electronic configuration and should, therefore, be a general feature for all ions.

As can be seen from Eqs. (5) and (6) the total coupling depends, in addition to the electronic states, on the properties of the vibrational eigenvectors ζ_k. The vibrational eigenvectors for a lattice containing a pseudolocalized mode can be subdivided into two parts[2]

$$\zeta_k=\eta_k+\mathbf{w}_k, \quad (10)$$

[12] G. H. Dieke, H. M. Crosswhite, and B. Dunn, J. Opt. Soc. Am. **55**, 820 (1961).
[13] B. R. Judd, Phys. Rev. **127**, 750 (1962).
[14] K. Rajnak, J. Chem. Phys. **37**, 2440 (1962).
[15] A. J. Freeman and R. E. Watson, Phys. Rev. **127**, 2058 (1962).

where η_k refers to the normal, plane-wave, phonon solutions of wave vector k of the undisturbed lattice, and $\mathbf{w}_k$ is the amplitude of the vibrational wave scattered at the defect. Within the frequency range of a scattering resonance the vibrational amplitudes of the ions in the vicinity of the defect considerably exceed $|\eta_k|$,[16] which latter we may suppose normalized to unity. Because the eigenvectors ζ_k obey a closure property at any point in the lattice,[2] there must exist frequencies other than those near the resonance frequency, for which the local amplitude is less than $|\eta_k|$. Similarly, since the eigenvectors are normalized over the volume of the crystal,[2] those which possess high amplitudes at the defect must have amplitudes less than $|\eta_k|$ elsewhere, and conversely for those of low local amplitude. A more complete description of the eigenvectors ζ_k depends critically on the nature of the defect and that of the lattice, and is difficult to present in simple analytical forms, although it has been given in tabular form for simple lattices.[17] For the present purposes it suffices to make the following crude approximation. Near the resonance frequency and in the vicinity of the defect $|\mathbf{w}_k| \gg |\eta_k|$, so that we may approximate $|\zeta_k|$ by $|\mathbf{w}_k|$. Since there exist many more modes outside than within the range of the resonance frequency, we may assume that the amount each of these is depressed below $|\eta_k|$ in the vicinity of the defect is small. We therefore make the approximation that for these nonlocal modes $|\zeta_k| \approx |\eta_k|$.

Near the resonance frequency it is possible to evaluate the radial dependence of the magnitude of the scattering amplitude $|\mathbf{w}_k|$ in terms of the Green's function $G_l(\omega^2)$ of the problem.[2] This has been done here for a simple cubic monatomic lattice with a Debye density

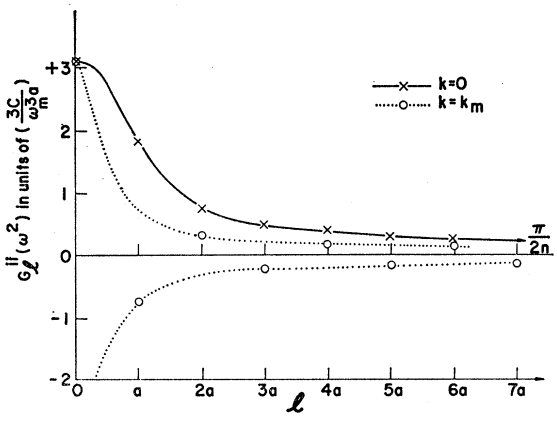

FIG. 5. Radial dependence of the amplitude of the Green's function of a simple cubic monatomic lattice evaluated at the center of and at the boundary of the Brillouin zone, i.e., at $k=0$ and at $k=\pi/a$.

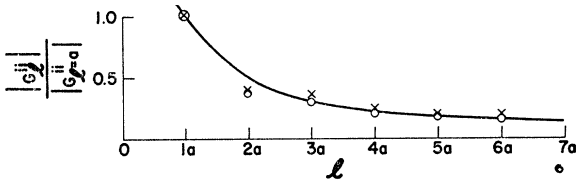

FIG. 6. Radial dependence of the amplitude of the Green's function normalized to its value at $r=1$ interatomic distance. The solid line is the function $f(\mathbf{l})=a/l$.

of states, for which we assume that the vibrational frequency $\omega=ck$. The Green's function is defined at the lattice sites which are enumerated by the position vector $\mathbf{l}$. Suppose we evaluate G_1 along a [100] direction of the cubic lattice, i.e., at the points $\mathbf{l}=0, a, 2a, 3a, \cdots, na$. This may be done simply at the center and at the boundary of the Brillouin zone, i.e., for values of ω for which $k=0$, and $k=k_m=\pi/a$. The result is shown in Fig. 5. The solid line in Fig. 5 shows that for $k=0$, the Green's-function amplitude (and therefore that of the scattering amplitude) is all of one sign, and decreases monotonically with distance from the defect. For $k=k_m$ the sign of the amplitude changes between neighboring ions (as we would have expected from the corresponding phonon solutions) and also decreases monotonically. If one normalizes the value of G_1 to its value not at the origin but to the value at $\mathbf{l}=a$ and takes the absolute value of this fraction, then one obtains for both $k=0$ and $k=k_m$ the points shown in Fig. 6. The solid line in Fig. 6 is the function $f(\mathbf{l})=a/l$. At the center and at the boundary of the first Brillouin zone one therefore finds that the local vibrational eigenvectors in the vicinity of a pseudolocalized oscillator decrease as $\mathbf{l}^{-1}$ for distances greater than one interatomic distance. We may safely assume that essentially the same dependence on $\mathbf{l}$ exists for other values of ω as well as for other simple lattices, although of course for these the phase relationship between the motion of neighboring ions may well vary.

It is now possible to calculate the linear coupling by carrying out the summation (4) over all the ions of the lattice except the defect ion at the origin. For simplicity we will assume that the coupling field $\mathbf{F}(\mathbf{R}_l)$ and the eigenvectors ζ_k have no angular dependence. In carrying out the summation over $\mathbf{l}$, we must remember that the number of ions (in a simple cubic lattice) in a differential volume of the crystal increases as $l^2/a^3 dl$, where a is the interatomic distance. The summation can be easily performed at the center and at the boundary of the Brillouin zone if we assume that the summation (4) can be replaced by an integration over $\mathbf{l}$. Further we separate the coupling into two parts, one for which the $\mathbf{F}(\mathbf{R}_l)$ is expandable in the pseudolocalized modes, and one for which the field is expandable in the nonlocalized modes. We investigate the sample case of acoustic motion, so that we approximate the nonlocalized modes, as noted above, by η_k

[16] P. G. Dawber and R. J. Elliott, Proc. Roy. Soc. (London) A273, 222 (1963).

[17] A. A. Maradudin, E. W. Montroll, G. H. Weiss, R. Herman, and H. W. Milner, Acad. Roy. Belg., Classe Sci., Mem.: Collection in 4°, 14, 7 (1960).

TABLE V. Linear coupling (in units of $\rho eZ/a^3N^{1/2}$).

Field	Vibrations	Linear coupling up to $\mathbf{l}=na$ $k=0$	Linear coupling up to $\mathbf{l}=na$ $k=\pi/a$	Total coupling $k=0$	Total coupling $k=\pi/a$
Dipole	Pseudolocalized	$(3\pi c/2a\omega_m{}^3)[1-1/n]$	$(3\pi c/4a\omega_m{}^3)$ $\times[1+(-1)^n/n+\pi(\mathrm{Si}\pi-\mathrm{Si}\pi)]$	$3\pi c/2a\omega_m{}^3$ [a]	$(3\pi c/2a\omega_m{}^3)$ (0.03)
Dipole	Nonlocalized	$\ln n$	$\mathrm{Ci}\pi n-\mathrm{Ci}\pi$	see Ref. 18	0.08
Quadrupole	Pseudolocalized	$(3\pi c/4a^2\omega_m{}^3)[1-1/n^2]$	$(3\pi c/4a^2\omega_m{}^3)$ $\times[1+(-1)^n/n+\pi^2(\mathrm{Ci}\pi n-\mathrm{Ci}\pi)]$	$(3\pi c/4a^2\omega_m{}^3)$	$(3\pi c/4a^2\omega_m{}^3)$ (0.21)
Quadrupole	Nonlocalized	$(1/a)[1-1/n]$	$(1/a)$ $\times[1+(-1)^n/n+\pi(\mathrm{Si}\pi n-\mathrm{Si}\pi)]$	$1/a$	$(1/a)$ (0.06)

[a] $3\pi c/2a\omega_m{}^3$ is roughly of unit magnitude for typical ionic crystals.

so that in $\boldsymbol{\eta}_k$ the polarization vectors have unit amplitude and lie in the propagation direction, but that the phase factor varies as $\exp[ikl]$. The linear coupling is then simply

$$\frac{1}{a^3}\int_l (\mathbf{F}(\mathbf{R}_l)\cdot\boldsymbol{\zeta}_k)l^2dl,$$

where $\mathbf{F}(\mathbf{R}_l)$ is proportional to l^{-3} or l^{-4} depending on whether we are considering dipole or quadrupole fields, respectively, and $\boldsymbol{\zeta}_k$ is proportional to l^{-1} or e^{ikl} for pseudolocalized modes and nonlocalized modes, respectively.

The physically significant values, as far as the present experimental results are concerned, are of course the asymptotic values of the above integral, which we will call the total linear coupling, and the rate of approach at which this asymptotic value is reached. The latter we determine by integrating from $l=0$ to arbitrary values of l. The result is given in the first two columns of Table V for vibrational modes near the center of the zone and at the boundary, i.e., at $k=0$ and $k=\pi/a$. The coupling has been evaluated at the lattice sites defined by $l=na$, where $n=1, 2, 3, \cdots$. The values listed in Table V must be multiplied for each electronic state by the coefficients of r^{-3} and r^{-4} given in Table IV for dipole and quadrupole fields, respectively. In the last two columns of Table V we list the asymptotic values of the integral, i.e., the total linear coupling.[18]

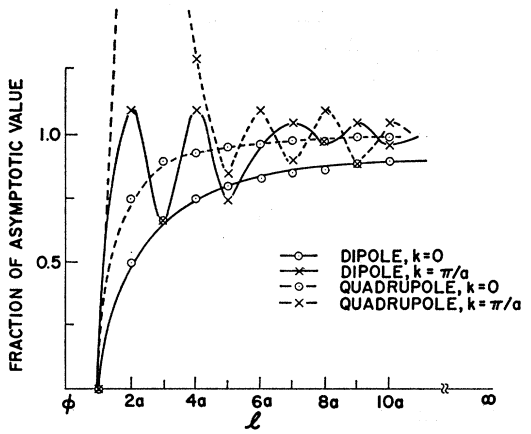

FIG. 7. Rate of approach to the asymptotic value of the dipole and quadrupole coupling to pseudolocalized vibrations for $k=0$ and $k=\pi/a$.

A number of features of Table V should be noted. For quadrupole fields the approach to the asymptotic value is more rapid than for dipole fields. This is illustrated in Fig. 7 for coupling to pseudolocalized modes. Figure 7 also illustrates the general feature that near the zone boundary the coupling magnitude is a rapidly oscillating function of $\mathbf{l}$. The asymptotic values for $k=\pi/a$ are smaller than those for $k=0$ by factors of 10^{-1} to 10^{-2}, as would be expected from the rapidly oscillating nature of G_1, while the rate of approach to the asymptotic value is essentially the same for both values of k.

For coupling to pseudolocalized modes, the fastest approach to the asymptotic value is that for quadrupole fields which approach the asymptotic value as l^{-2}, i.e., at a faster rate than the decrease in the amplitude of the local vibration which decreases as l^{-1} (see Fig. 6). The asymptotic value for dipole coupling is reached at the same rate as the decrease in the enhanced local vibrations. The dipole coupling to the nonlocalized modes also extends over a large region of the crystal approaching the asymptotic value approximately as $\ln l$. The quadrupole coupling, in comparison, decreases as l^{-1}. One reaches, therefore, the conclusion that the dipole coupling extends over the entire crystal and considerably exceeds the radial extent of the quadrupole coupling, the latter being limited to the vicinity of the defect.

C. Comparison with Experimental Results

Case I. No Inversion Symmetry

We now apply these findings to the case of Sm^{2+} in the alkali halides. In this lattice, the Sm^{2+} ion has as a nearest neighbor, in a [110] direction, a positive-ion vacancy which is required for charge compensation.

[18] The asymptotic value for dipolar coupling to nonlocalized modes is finite for finite values of k. As $k\to 0$, the asymptotic value appears to diverge to infinity. This apparent unrealistic result can be treated in a manner similar to that proposed by A. A. Maradudin and G. H. Weiss, Phys. Rev. **123**, 1968 (1961) and T. H. K. Barron, *ibid.* **123**, 1995 (1961) for the limiting optical frequency in ionic crystals.

TABLE VI. Comparison of peak position of vibronic structure and singularity points in dispersion curves of KBr; (frequencies in units of 10^{12} sec^{-1}).

Peak designation	Frequency from vibronic structure	Designation of critical points		
		Symmetry point or line	Branch[a]	Frequency
A	1.26	X	TA	1.25
		L	TA	2.20
B	2.21	X	LA	2.15
C	2.57	Δ(at $\zeta \approx 0.6$)	LA	$\sim$2.68
D	3.18	L	TO	3.06
E	3.57	$\Delta+X$	TO	3.65
F	4.38	L	LO	4.34

[a] TA = transverse acoustic, LA = longitudinal acoustic, TO = transverse optic, LO = longitudinal optic.

The point group of the site of the Sm^{2+} ion is C_{2v}, i.e., it lacks inversion symmetry,[8] and all its states are nondegenerate. Accordingly, the linear coupling for intraconfiguration transitions and that for interconfiguration transitions is given by Eq. (8).

Interconfiguration transitions are observed in absorption spectra from the ground electronic state $^7F_0(A_1)$ to unknown states of the $4f^5 5d$ and other higher excited configurations. Although little is known about the terms of these excited configurations, we do know from Sec. IIIB that the transition may involve a strong change in the equilibrium value of the normal coordinates of vibration,[19] primarily because of the large change in the quadrupole coupling fields as shown in Table IV. The change in the dipole coupling is smaller, due to the inherently smaller dipole field, and because only a small fraction, $\langle \psi_j | V_c | \psi_B \rangle / \Delta E$, of the states $\psi_j(\alpha)$ is admixed. For Sm^{2+} we estimate this fraction to be of the order of 10^{-1} to 10^{-2} for the lowest energy states of the $4f^5 5d$ configuration. The quadrupole coupling involves primarily the ions in the immediate neighborhood of the Sm^{2+}. Since these have enhanced amplitudes in the frequency range of the pseudolocalized resonance vibrations,[2] the resultant vibronic spectra is dominated by the relatively sharp lines from transitions to electronic states with simultaneous emission (or absorption) of quanta of the pseudolocalized vibrational modes. Since α_κ may also be large, according to Eq. (3) multiquanta transitions have finite transition probabilities, so that one observes long series of vibronic lines as shown in Fig. 4.

It has been shown in Ref. 1 that for Sm^{2+} in the alkali halides the quadrupole coupling is limited to vibrations of the unit representation, i.e., of the A_1 representation of C_{2v}.[20] It has also been shown that besides two strong resonance vibrations (ω_1 and ω_2 of Fig. 4), there exist other locally increased vibrations, however, with reduced amplitudes. These latter contribute to the background observed in the spectrum of Fig. 4 (see also Fig. 1 of Ref. 1). The much weaker dipolar coupling also contributes to the background spectrum. The dipolar coupling, as noted above, overlaps the vibrations of both local ions and the ions in more extended regions of the crystal. Since there are, however, many more nonlocal modes than pseudolocalized modes, the dipolar coupling is dominated by the nonlocal vibrations. It can be shown for Sm^{2+} in the alkali halides that the dipolar coupling is also limited to vibrations of A_1 type, as long as the electronic states are mixed only by a static crystal field.

For intraconfiguration transitions, the two quadrupole coupling terms in Eq. (8) may in general either partly cancel or add depending on the particular electronic states. In any event, the magnitude of the quadrupole coupling will be smaller than for interconfiguration transitions, due to the reduced quadrupole coupling field. The dipole term remains, in general, a small term compared to the quadrupole term.

The intraconfiguration transition $^5D_0(A_1) \rightarrow {}^7F_0(A_1)$ of Sm^{2+} in the alkali halides is a special case, since the quadrupole coupling vanishes. This results from the fact that the $4f$ components of these states i.e., $\psi_B(\alpha)$ and $\psi_A(\alpha)$, are spherically symmetric, and therefore have no multipole fields. Only the dipole coupling term of Eq. (8) contributes to α_κ, and since the latter is very small, zero- and one-quantum vibrational processes can at best be observed experimentally. The dipole coupling as noted above, is dominated by the nonlocal vibrations, so that the vibronic spectrum reflects the A_1 vibrations of the nonlocalized modes.

We expect, therefore, that the vibronic structure of Figs. 1, 2, and 3 approximates the density of phonon states with A_1 symmetry. The density of states can, in principle, be calculated for KBr from the dispersion curves obtained by Woods *et al.*[7] from neutron-scattering data. From the dispersion data and the shell model a representative set of eigenvectors over the first Brillouin zone can be obtained, and the components of these on nonlocalized and pseudolocalized modes of A_1 symmetry determined. This rather detailed calculation which would, in any event, extend unduly the

[19] As shown in Ref. 1, the displacement in the equilibrium position can, in principle, be obtained from the structural form of the vibronic spectra. The displacement is found to depend on the host lattice.

[20] This follows directly from the fact that the symmetric product $[\psi_j \times \psi_j]$ must be the unit representation when all ψ_j are one dimensional, and from the fact that U_κ must be a basis for the representation κ in r space.

present paper, we defer for possible future work. Instead, we limit ourselves here to a qualitative correlation between the peaks in the vibronic structure, as given in Table I, and the critical points (where $\nabla_\kappa\omega=0$) in the dispersion curves for KBr.

Loudon[21] has recently given the phonon symmetries of the NaCl-type lattice and their reduction to the point-group symmetries of the lattice. The latter may be readily further reduced to the C_{2v} group of the site of the Sm^{2+} ion. Using Table I of Loudon's paper, it can be shown that all phonon branches at the special symmetry points and lines contain the A_1 (totally symmetric) point-group representation. If one compares the frequencies of the peaks as given in Table I with the frequencies at the critical points in the dispersion curves of Woods *et al.*, one obtains the assignments given in Table VI. The agreement between the two sets of values is very good. Particular note should be taken of the location of the gap between the acoustical and optical branch which appears in Fig. 3 at 2.94×10^{12} sec^{-1} and which has been calculated from the neutron-scattering data by Cochran *et al.*,[22] to be at 2.9×10^{12} sec^{-1}. Despite this apparent agreement, the validity of the assignments of Table VI are limited by a number of factors. Woods *et al.* have given dispersion curves for KBr only for the [100], [110], and [111] directions in **k** space. Thus the contribution to the density of states from other directions and symmetry points, such as the point W, have been left out. The dispersion curves are reported from neutron-scattering data taken at 90°K, whereas the optical data given here were taken at 10°K. No attempt has been made to correct for this change in temperature. The strength of the singularities at the various critical frequencies has not been checked.[23] Also, the distorting effect of the pseudo-localized vibrations on the density of states has not been evaluated. It must be emphasized, therefore, that the assignments of Table VI are tentative until the more detailed calculations described above are made.

Case II. Inversion Symmetry

The case of inversion symmetry is complicated since for it, it is no longer realistic to limit oneself to nondegenerate states as has been assumed so far. Consequently, $\langle\psi_j|U_\kappa|\psi_j\rangle$ will now, in general, be nonzero for modes κ other than the unit representation. Because there is now a coupling to vibrational modes that destroy the initial symmetry, the electronic levels will not remain degenerate and a Jahn-Teller splitting of the states can be expected. It is not clear at this time how this complication affects the perturbation treatment used to obtain Eq. (9) or how it affects the assumption, inherent in the electrostatic-coupling model, that the change in the repulsive part of the electron-lattice interaction potential $U(r,Q)$ between two states is of lower order than the change in the electrostatic interaction.

An exception to the above complication is the vibronic structure accompanying the (forbidden) intraconfiguration transition between the nondegenerate states $^5D_0(A_{1g})$ and $^7F_0(A_{1g})$ in Sm^{2+} in the alkaline-earth halides. This structure was first reported by Wood and Kaiser,[4] and has been discussed by Axe and Sorokin[3] and by Richman.[24] Equation (9) predicts the vibronic structure accompanying transitions between two nondegenerate electronic states. If the quadrupole coupling differs in the two electronic states A and B, then α_κ is finite and multiquanta vibrational transitions become possible. However, the first term of (9) does not lead to an observable spectrum since $\langle\psi_{j'}{}^0(\alpha)|P_\epsilon|\psi_j{}^0(\alpha)\rangle$ vanishes. However, the second term in (9) predicts that simultaneous emission (or absorption) of quanta of even vibrational modes and one quantum of an odd vibrational mode can be observed. The latter, the so-called "forced electric-dipole transitions,"[25] can be observed since, in general, $\langle\psi_j(\alpha)|P_\epsilon|\psi_j(\alpha')\rangle$ is finite. The coupling to the odd vibrations involves the dipole coupling fields which result, as noted above, in a vibronic structure which approximates the density of states of the vibrations of the undisturbed lattice. The vibronic structure for case II, therefore, most likely consists of overlapping series of bands representative of the density of states of nonlocal vibrations.

For the special case of the transition $^5D_0(A_{1g})\rightarrow{}^7F_0(A_{1g})$ the quadrupole contribution again vanishes, so that α_κ goes to zero. For this case, Eq. (9) reduces to that treated by Satten,[25] for which only transitions involving a change of one quantum of the odd vibrational modes are allowed. It can readily be shown[3] that this transition involves only those phonons which contain the T_{1u} point-group representation. According to Loudon, this can include the phonons at Γ_{15}^-, X_4^-, $X_5^-(2)$, $W_2'(2)$, and $W_3(2)$. (The number in parentheses refers to the number of branches in which the point occurs.) At Γ_{15}^-, which is at $k=0$, the density of phonon states goes to zero; therefore these phonons will not contribute to the vibronic structure. It should be possible to check the above prediction, and thereby the formulation (9), when the dispersion curves and band-structure calculations for the alkaline-earth halides become available.

Most of the published vibronic spectra accompanying intraconfiguration transitions for the case II appear to be limited to one-phonon transitions. This would seem to indicate, the perhaps reasonable result, that the change in the quadrupole coupling between states of the same configuration is generally small, so that α_κ is

[21] R. Loudon, Proc. Phys. Soc. (London) **84**, 379 (1964).
[22] R. A. Cowley, W. Cochran, B. N. Brockhouse, and A. D. B. Woods, Phys. Rev. **131**, 1030 (1963).
[23] L. Van Hove, Phys. Rev. **89**, 1189 (1953).
[24] I. Richman, Phys. Rev. **133**, A1364 (1964).
[25] J. H. Van Vleck, J. Phys. Chem. **41**, 67 (1937); R. A. Satten, J. Chem. Phys. **27**, 286 (1957); **29**, 658 (1958); **30**, 590 (1959).

small. The vibronic structure recently reported by Kiss[26] for the transitions $7T_1^{(2)} \rightarrow 8E^{(2)}$ and $7T_1^{(1)} \rightarrow 8T_2^{(2)}$ of Dy^{2+} in CaF_2 and SrF_2 may be an indication, however, that α_κ need not always be small.

[26] Z. J. Kiss, Phys. Rev. 137, A1749 (1965).

ACKNOWLEDGMENTS

The author is deeply indebted to Dr. J. D. Axe and Dr. T. D. Schultz for many helpful discussions, and to Dr. M. Wagner, whose work forms the basis for most of the content of this paper.

PHYSICAL REVIEW VOLUME 140, NUMBER 6A 13 DECEMBER 1965

Thermal Conductivity of Electron-Irradiated Silicon*

FREDERICK L. VOOK
Sandia Laboratory, Albuquerque, New Mexico
(Received 23 July 1965)

Changes in the low-temperature thermal conductivity of single-crystal Si were investigated upon 2-MeV electron irradiation and annealing. The additive thermal resistivity of high-purity p-type Si irradiated below 60°K to maximum time-integrated fluxes Φ of 8.0×10^{18} 2-MeV e/cm^2 increases as $1/K-1/K_0 = 3.75\times10^{-13}\,\Phi^{0.61}$ cm-deg/W at 47°K. The $\Phi^{0.61}$ dependence of the additive thermal resistivity of Si on bombardment is very similar to the $\Phi^{0.58}$ dependence previously observed for Ge. The magnitude of the increase is, however, much smaller than previously observed for either Ge, InSb, or GaAs. The linear concentration dependence of GaAs has been related to mass-difference strain-field scattering, whereas the nonlinear concentration dependencies of InSb, Ge, and Si suggest phonon-electron scattering. For the high-purity Si, annealing begins near 80°K, and exhibits a single dominant annealing stage near 140°K corresponding to the annealing temperature of vacancies in p-type Si. Measurements of the temperature dependence of the thermal conductivity indicate that the defects anneal primarily as point defects, although evidence exists for a small amount of precipitation of point defects in the annealing-temperature interval between 80 and 135°K. Sharp minima observed in the temperature dependence of the thermal conductivity of Si are similar to those previously observed in Ge and attributed to resonant scattering.

I. INTRODUCTION

ALTHOUGH electron spin resonance measurements by Watkins[1] have established that vacancies move and interact with impurities[1–3] at low temperature in silicon, there have been very few investigations of the effects on other physical properties of the low-temperature introduction and annealing of lattice defects. Such investigations must be conducted with the realization that the motion of the vacancy at 65°K in n-type Si[1] and near 140°K in p-type Si,[2] leads to interactions with chemical impurities well below room temperature[3] and greatly complicates measurements at higher temperatures.[4] Primary defects must therefore be studied in high-purity silicon irradiated at low temperature.

Electrical measurements are difficult to perform in irradiated high-purity Si at low temperature, and therefore very few exist.[5,6] However, low-temperature thermal conductivity has been shown to be highly sensitive to lattice defects introduced into high-purity GaAs,[7] InSb,[8] and Ge,[9] by electron irradiation. It has also been shown that measurements of the temperature dependence of the low-temperature thermal conductivity on annealing are related to changes in the structural properties of the defects and are therefore useful in distinguishing between the annealing behavior of radiation-induced defects in different semiconductors. Precipitation in GaAs[7] of point defects introduced by electron irradiation is in contrast to the almost complete recovery and annihilation of similar point defects introduced in Ge.[9] In addition, the increase in low-temperature thermal resistivity on electron irradiation can be related to theories of phonon scattering, and the magnitude and kind of such scattering can differ greatly from one semiconductor to another. For these reasons, changes in the thermal conductivity of Si upon electron irradiation were investigated.

* This work was supported by the U. S. Atomic Energy Commission.

[1] A recent review of the spin resonance centers in Si is given by G. D. Watkins, *Proceedings of the 7th International Conference on the Physics of Semiconductors. 3. Radiation Damage in Semiconductors* (Dunod Cie, Paris, 1965), p. 97.

[2] G. D. Watkins, J. Phys. Soc. Japan 18, Suppl. II, 22 (1963).

[3] G. D. Watkins, J. W. Corbett, and R. M. Walker, J. Appl. Phys. 30, 1198 (1959); G. D. Watkins and J. W. Corbett, Phys. Rev. 121, 1001 (1961); J. W. Corbett, G. D. Watkins, R. M. Chrenko, and R. S. MacDonald, *ibid.* 121, 1015 (1961); G. D. Watkins and J. W. Corbett, *ibid.* 134, A 1359 (1964).

[4] Y. Inuishi and K. Matsuura, J. Phys. Soc. Japan 18, Suppl. III, 240 (1963).

[5] G. K. Wertheim and D. N. Buchanan, J. Appl. Phys. 30, 1232 (1959).

[6] V. S. Vavilov and A. F. Plotnikov, J. Phys. Soc. Japan 18, Suppl. III, 230 (1963); V. S. Vavilov, *Proceedings of the 7th International Conference on the Physics of Semiconductors. 3. Radiation Damage in Semiconductors* (Dunod Cie, Paris, 1965), p. 115.

[7] F. L. Vook, Phys. Rev. 135, A1742 (1964).

[8] F. L. Vook, Phys. Rev. 135, A1750 (1964).

[9] F. L. Vook, Phys. Rev. 138, A1234 (1965).